JACS
JOURNAL OF THE AMERICAN CHEMICAL SOCIETY

Article

pubs.acs.org/JACS

The Synthesis of Cyclic Poly(ethylene imine) and Exact Linear Analogues: An Evaluation of Gene Delivery Comparing Polymer Architectures

Mallory A. Cortez,[†] W T. Godbey,[‡] Yunlan Fang,[‡] Molly E. Payne,[§] Brian J. Cafferty,[§] Karolina A. Kosakowska,[§] and Scott M. Grayson*[,§]

[†]Department of Physical Sciences, Nicholls State University, Thibodaux, Louisiana 70310, United States

[‡]Department of Chemical and Biomolecular Engineering, Tulane University, New Orleans, Louisiana 70118, United States

[§]Department of Chemistry, Tulane University, New Orleans, Louisiana 70118, United States

Supporting Information

ABSTRACT: The delivery of genetic material to cells offers the potential to treat many genetic diseases. Cationic polymers, specifically poly(ethylene imine) (PEI), are promising gene delivery vectors due to their inherent ability to condense genetic material and successfully affect its transfection. However, PEI and many other cationic polymers also exhibit high cytotoxicity. To systematically study the effect of polymer architecture on gene delivery efficiency and cell cytotoxicity, a set of cyclic PEIs were prepared for the first time and compared to a set of linear PEIs of the exact same molecular weight. Subsequent in vitro transfection studies determined a higher transfection efficiency for each cyclic PEI sample when compared to its linear PEI analogue in addition to reduced toxicity relative to the branched PEI "gold standard" control. These results highlight the critical role that the architecture of PEI can play in both optimizing transfection and reducing cell toxicity.

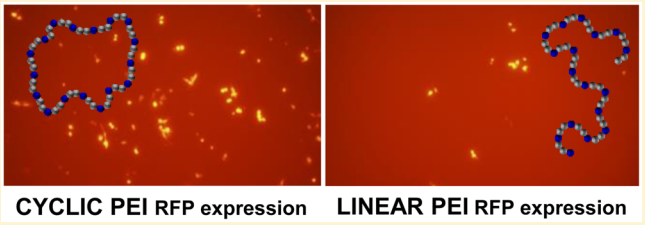

INTRODUCTION

Fundamentally, gene therapy involves the expression of exogenous DNA, which relies upon the successful transport of intact DNA into the nuclei of the target cells. Gene therapy offers promise to manage or possibly cure many genetic disorders in which a malfunctioning gene is attenuated by a "healthy" exogenous gene.[1,2] Gene therapy also has been probed for use in disease prevention, such as vaccinations, as well as anticancer therapies.[2−9] Because of the poor stability of DNA in vivo, appropriate vectors are required to protect the genetic payload during transport, as well as affect its delivery across the cell membrane and into the nucleus. While viral capsids represent attractive vectors due to their high efficiency, concerns exist about their immunogencity[10,11] and their cost.[6] Cationic polymer vectors have emerged as a promising alternative because of their scalable production, as well as synthetic ease of tuning their size, structure, and functionality. While a number of amine-containing, cationic polymers have been explored, including poly(ethylene imine) (PEI),[12] poly-L-lysine (PLL), poly(2-(dimethylamino)ethyl methacrylate) (PDMAEMA), and polyamidoamine (PAMAM) dendrimers, nonviral gene delivery still suffers from lower transfection efficiencies when compared to viral capsids and high cytotoxicity attributed to their polycationic character.[2,6,13,14]

Of these polymeric carriers, PEI-based polymers remain one of the most successful classes of synthetic vectors for gene transfection.[12] At physiological pH, the cationic backbone of the polymer efficiently complexes with the anionic phosphates of DNA; however, such polycations also exhibit cytotoxicity.[2,15] As a result, amine-rich polymers have been the subject of numerous studies aimed at understanding the relationship between structural parameters, such as molecular weight, degree of branching, amine spacing, and amine number on DNA/polymer complexation potential, transfection efficiency, and cytotoxicity.[13,14,16−23]

Though much research with PEI has shown that the molecular weight is a critical parameter for optimizing gene delivery,[16,18−23] truly systematic studies of PEI architectural effects on transfection efficiency and cytotoxicity remain wanting. This neglect is largely a consequence of the synthetic challenge in preparing PEI libraries in which the architecture is varied systematically yet the amine composition (e.g., primary vs secondary or tertiary) and molecular weight remain the same. Without access to such architectural analogues, it is difficult to draw meaningful conclusions as to the specific relationship between macromolecular structure and biological activity. For example, there is still some debate as to whether branched PEI shows higher transfection efficiency than linear PEI; this comparison is complicated because of the multiple parameters which are changed, including the substitution of the amines, the absolute molecular weight, the molecular weight

Received: January 28, 2015
Published: April 30, 2015

DOI: 10.1021/jacs.5b00980
J. Am. Chem. Soc. 2015, 137, 6541−6549

dispersity of the sample, the charge density/compactness and the structural flexibility, as well as the degree of branching.

In one of the more systematic studies addressing the effect of polymer architecture on gene transfection, Tang et al.[14] studied whole PAMAM dendrimers relative to degraded PAMAM dendrimers for use as gene delivery agents. The partially degraded PAMAM dendrimers exhibited better transfection efficiency than the parent nondegraded dendrimers or highly degraded dendrimers. While additional reports exist for the gene delivery capabilities of well-defined nonlinear polymers such as dendrimers[24] and star polymers,[25−28] truly systematic comparisons remain rare. Herein, we explore the properties of two PEI polymers that contain the same number and type of amines, but differ only in their architecture. This has been carried out by preparing for the first time well-defined cyclic PEIs as well as their exact linear analogues.

Cyclic polymers exhibit unique physical properties owing to their unusual topology, but detailed studies have been limited due to technical difficulties in preparation and purification.[29−33] Cyclic macromolecular topologies also impart unique and potentially useful biological properties. For example, Szoka and co-workers demonstrated that cyclic polymer scaffolds exhibit increased blood circulation times in vivo[34] and also yield greater tumor accumulation than their linear polymer counterparts.[35] Recently, a versatile cyclization method utilizing the highly efficient copper-catalyzed azide−alkyne cycloaddition (CuAAC) reaction has been developed to yield a range of high purity cyclic polymers, including polystyrene,[36] polyesters,[37] and block copolymers.[38] This route offers synthetic access to a wide variety of cyclic macromolecules to enable their evaluation for numerous applications. Recent studies of cyclic PDMAEMA has suggested that cyclic polymers have advantages for nucleic acid delivery.[39]

To investigate the utility of cyclic PEI for gene delivery, linear poly(2-ethyl-2-oxazoline) (PEOx) precursors[40−42] were prepared via the ring-opening polymerization of 2-ethyl-2-oxazoline such that azide and alkyne functionalities were located at opposite ends of the polymer chain. Utilization of the CuAAC cyclization technique provided cyclic PEOx samples with the identical molecular weight as their linear precursors.[43] The acid-catalyzed hydrolysis of these cyclic and linear PEOx sets therefore provided access to a library of cyclic and linear PEI samples that were subsequently investigated as vehicles for the delivery of plasmids encoding red fluorescent protein (RFP).

EXPERIMENTAL SECTION

Polymerization of PEOx.[44] PEOx was polymerized with either propargyl *p*-toluenesulfonate or methyl *p*-toluenesulfonate in a CEM microwave reactor at varying initiator to monomer ratios. NaN_3 was added to the reaction mixture to terminate the polymer chains with an azido functionality. The PEOx was purified by precipitating into diethyl ether and washing with $NaHCO_3$.

Cyclization of PEOx. α-Alkynyl-ω-azido PEOx was dissolved in a flask containing 100 mL of $CHCl_2$, while in a separate 250 mL two-neck round-bottom flask equipped with a stir bar, *N*,*N*,*N*′,*N*″,*N*″-pentamethyldiethylenetriamine was dissolved into 120 mL of $CHCl_2$. Both reaction vessels were degassed three times via freeze−pump−thaw cycles after which time Cu(I)Br was added to the second flask while frozen. Once thawed, a syringe pump with a 25 mL gastight syringe was used to add the polymer/solvent solution to the 250 mL round-bottom flask containing the Cu(I)Br/PMDETA/$CHCl_2$ solution at a rate of 2 mL/h at room temperature. The reaction was then exposed to air, and washed multiple times with a saturated aqueous NH_4Cl solution to extract the copper salts. Removal of residual copper salts was performed by passing the polymer through a plug of silica with CH_3OH as the eluent. After drying in vacuo, the polymer was redissolved in THF, and the solution passed through a 13 mm GD/X disposable syringe filter (PTFE filter media; polypropeylene housing; 0.2 μm pore size). Representative yield: 85%.

CuAAC Conjugation for Linear Triazole Control PEOx. α-Methyl-ω-azido PEOx was added to a 250 mL two neck, round-bottom flask containing a magnetic stir bar and then dissolved in 150 mL of $CHCl_2$. *N*,*N*,*N*′,*N*″,*N*″-Pentamethyldiethylenetriamine (PMDETA) and propargyl alcohol were added to the reaction flask. The reaction vessel was then degassed three times via freeze−pump−thaw cycles during which time Cu(I)Br was added to the flask while frozen. Once thawed, the reaction was stirred overnight. Polymers were purified following the same procedure as described for cyclic PEOx. Representative yield: 97%.

Acid Hydrolysis of PEOx to PEI.[45] PEOx was dissolved in 5 M (16.8 wt %) aq. HCl and reacted under reflux for 24 h. The reaction was then cooled to room temperature, and the acid solution was removed in vacuo. Fresh deionized water was then added, and the solution was neutralized with 2.5 M NaOH solution to a pH >8. The precipitated PEI was then filtered, washed with DI water, dissolved in methanol, and precipitated in diethyl ether. Representative yield: 96.7%,

Cells and Media. Human foreskin fibroblasts (HFF-1) (ATCC, Manassas, VA) were cultured in Dulbecco's Modified Eagle Medium supplemented with 15% fetal bovine serum and 100 U/mL each of penicillin and streptomycin. Human aortic endothelial (HAE) cells (a kind gift from Dr. Tabassum Ahsan, Department of Biomedical Engineering, Tulane University) were cultured in EGM-2 Bullet Kit media (Lonza, Allendale, NJ). Both cell types were maintained at 37 °C, 5% CO_2, and saturated humidity.

Formation of Complexes for Gene Delivery. DNA solutions were prepared at a concentration of 72 μg/mL (1 dose of 3.6 μg/50 μL) in sterile 0.9% saline. PEI solutions, also in sterile 0.9% saline, were prepared at the N:P ratios to be tested, pH = 7, and filtered through 0.2-μm cellulose acetate. Polymer solutions were added to plasmid solutions to bring the final volumes of transfection solutions to 100 μL/dose, and used within 30 min for transfection.

Transfection Experiments. Cells were plated at 1×10^5 cells/well in 6-well plates 16 h prior to transfection. For transfection, media were replaced with 2 mL of serum-free versions plus 100 μL of PEI/DNA complexes. Cells were incubated at 37 °C for 4 h, after which the transfection medium was replaced with growth medium. Experimental results were collected at 24 h post-transfection. Expression of fluorescent reporters was determined via fluorescence microscopy, with transfection efficiency being defined as (no. of fluorescent cells counted/total cells counted). A minimum of 5 visual fields per well were counted to yield transfection efficiencies.

Viability Assay. Cells were transfected as described above, with the inclusion of a SHAM control. At 24 h post-transfection, growth media were removed and cells were washed twice with 1 mL of phosphate-buffered saline to remove nonadherent cells. A volume of 300 μL trypsin was added to each well to detach and isolate the remaining cells, followed by the addition of 300 μL of growth medium (with FBS) to each well. Media and cells were collected in polypropylene tubes, followed by the addition of the viability assay reagent (LIVE/DEAD Viability/Cytotoxicity Kit*, Invitrogen Life Technologies, Carlsbad, CA). The suspension was incubated in the dark for 15−20 min at room temperature. Cells were counted via hemocytometer. Percent viability was defined as (the number of live cells for the sample well/the number of live cells for the Sham well).

RESULTS AND DISCUSSION

To obtain well-defined sets of cyclic and linear PEI analogues, both were prepared directly from their *N*-acyl protected PEOx precursors. The presence of the acyl groups during polymerization prevents the occurrence of branching and assures that

DOI: 10.1021/jacs.5b00980
J. Am. Chem. Soc. 2015, 137, 6541−6549

Scheme 1. Synthetic Scheme for the Production of the Desired PEI Library Including Linear (3) and Cyclic (4) Plus a Linear Triazole Control (7) PEI[a]

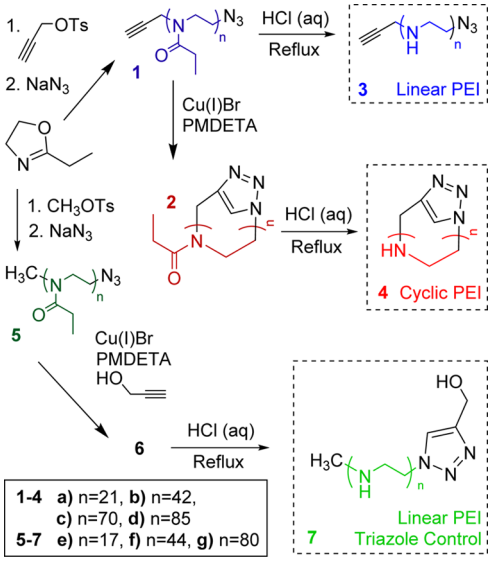

[a]PMDETA = *N,N,N′,N″,N″*-pentamethyldiethylenetriamine, Ts = tosylate.

Table 1. The Observed Average Molecular Weight, M_n, Dispersity, $Đ$, and Degree of Polymerization, DP, for the Library of Linear, Cyclic, and Linear Triazole Control Peox Polymers

	PEOx Precursors					PEI Products		
		M_n		$Đ$				
no.	M/I	GPC	MS	GPC	MS	no.	M_n[a]	DP
Linear Polymers								
1a	20	2100	2100	1.10	1.04	**3a**	970	21
1b	50	4100	4200	1.08	1.02	**3b**	1880	42
1c	80	7000	7000	1.05	1.02	**3c**	3080	70
1d	100	8500	8500	1.05	1.01	**3d**	3730	84
Cyclic Polymers								
2a	20	1700	2000	1.21	1.05	**4a**	970	21
2b	50	3400	4100	1.09	1.02	**4b**	1880	42
2c	80	4400	6900	1.04	1.02	**4c**	3080	70
2d	100	4500	8300	1.05	1.02	**4d**	3730	84
Linear Triazole Control								
6e	20	1700	1700	1.09	1.03	**7e**	850	17
6f	80	4500	4400	1.02	1.02	**7f**	2010	44
6g	100	7500	8000	1.03	1.01	**7g**	3560	80

[a]The average molecular weights and DP for the PEI products were determined from the PEOx MS data.

the backbone is composed exclusively of secondary amines after deacylation.

Linear PEOx Polymerization. With propargyl *p*-toluenesulfonate as the initiator, 2-ethyl-2-oxazoline was polymerized under anhydrous conditions in a microwave reactor. The use of a microwave reactor was found to increase the polymerization rate while minimizing termination and chain transfer reactions resulting from trace amounts of water. The polymerization reactions were terminated by the addition of sodium azide which quenched the propagating chain end to yield the linear PEOx, **1**, (Scheme 1), bearing one alkyne group and one azide group at opposite ends of the polymer chain. This polymerization was repeated at different initiator to monomer ratios to synthesize a series of linear PEOxs with molecular weights ranging from 2100 to 8500 (Table 1, **1a**−**1d**).

CuAAC Cyclization of Linear PEOx To Generate Cyclic PEOx. Although a number of techniques have been reported for preparing cyclic polymers,[30] the CuAAC cyclization method is particularly versatile because it is independent of the polymerization mechanism, requiring only the ability to install one alkyne group and one azide group at opposite chain ends. To ensure these complementary functional groups react in an intramolecular fashion to yield the desired cyclic product, the linear PEOx precursors, **1**, are added to the CuAAC catalyst via a slow dropwise addition, thus ensuring high dilution and nearly quantitative generation of the desired cyclic PEOx. After purification by a series of aqueous NH_4Cl washes and precipitation (to remove the copper salts) cyclic PEOx, **2**, was obtained with molecular weights ranging from 2100 to 8500 (Table 1, **2a**−**2d**).

Acid Hydrolysis To Generate Linear PEIs, Cyclic PEIs, and Linear PEI Triazole Controls. Acid hydrolysis using 5 M HCl easily removed the acyl side chains affording well-defined, unbranched PEI samples.[42,46] By utilizing the combination of PEOx[40−42,44,47−49] precursors and CuAAC cyclizations,[30,36] sets of linear and cyclic PEI (**3** and **4**, respectively) were generated that exhibit identical molecular weights as well as an identical number and type of amines along the backbone. The only structural differences between **3** and **4** are their architecture and end groups: **3** is linear with azide and alkyne end groups, while **4** is cyclic with no end groups and a triazole linkage. To isolate any effect that the azide, alkyne, or triazole functional groups may have on subsequent transfection studies, an additional "linear PEI triazole control", **7**, was prepared that utilizes the CuAAC reaction to generate a PEI bearing a triazole terminal group but without modifying its linear topology (Scheme 1, **5**−**7**). This linear PEI triazole control was prepared from a monoazide PEOx, **5**, which lacked the complementary alkyne end group.

CuAAC conjugation with a small molecule alkyne yielded the desired linear PEOx precursor, **6**, which upon deacylation yielded **7**, the desired control with a triazole end group.

Characterization and Structural Confirmation. All of the compounds synthesized were characterized with Infrared (IR) spectroscopy, Matrix-Assisted Laser Desorption−Ionization Time of Flight Mass Spectrometry (MALDI-ToF MS), Proton Nuclear Magnetic Resonance (^{1}H NMR), Carbon Nuclear Magnetic Resonance (^{13}C NMR), and Gel Permeation Chromatography (GPC) to confirm their structure and molecular weight.

For the linear PEOx precursors, **1**, the IR spectrum exhibited the characteristic signal at 2100 cm^{-1} of the azide end group[45] (Supporting Information Figure S1a) while ^{1}H NMR and ^{13}C NMR analysis confirmed the expected resonances for the repeating units (Supporting Information Figures S2 and S6a). MALDI-ToF MS confirmed the PEOx repeating unit mass of 99.07 Da (observed mass 99.07 Da) while MS end group analysis revealed two distributions of signals: the expected distribution of the potassium adduct of **1**, and a second, stronger, metastable distribution (loss of N_2) that is characteristic of a polymer bearing a single azide functionality[50] (Figure 1a). MALDI-ToF MS analysis also provided a molecular weight determination of 2100 Da that agreed closely with GPC data (2100 Da). Molecular weight calculations (2000 Da) from ^{1}H NMR (end group at 4.1−4.2 ppm, Supporting Information

DOI: 10.1021/jacs.5b00980
J. Am. Chem. Soc. 2015, 137, 6541−6549

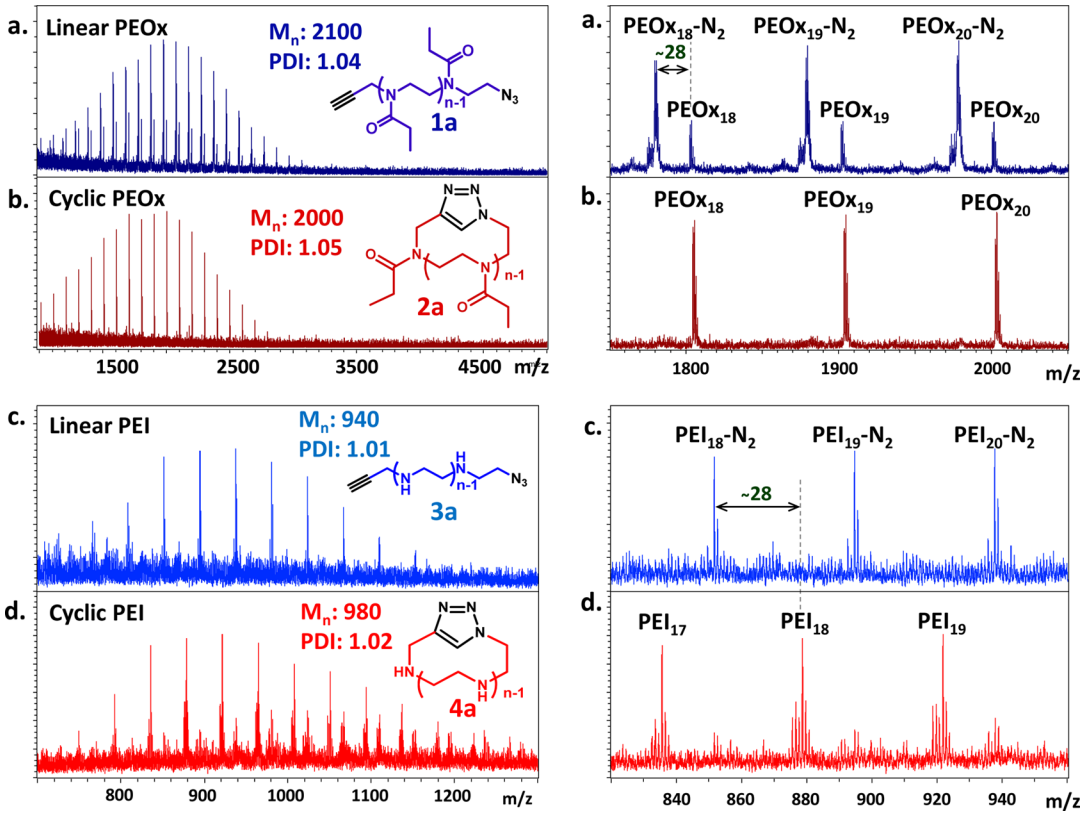

Figure 1. MALDI-ToF mass spectra of (a) linear PEOx (**1a**), (b) cyclic PEOx (**2a**), (c) linear PEI (**3a**), and (d) cyclic PEI (**4a**). The reflector mode mass spectra of linear polymers, **1a** (a) and **3a** (c) show the characteristic metastable fragmentation of the azide end group (via loss of N_2) as the major distribution.[50] For the cyclic polymers, **2a** (b) and **4a** (d), the disappearance of the azide metastable signals provides strong evidence for a nearly quantitative cyclization. K^+ adducts are observed for **1a** and **2a**, while H^+ adducts are observed for **3a** and **4a**.

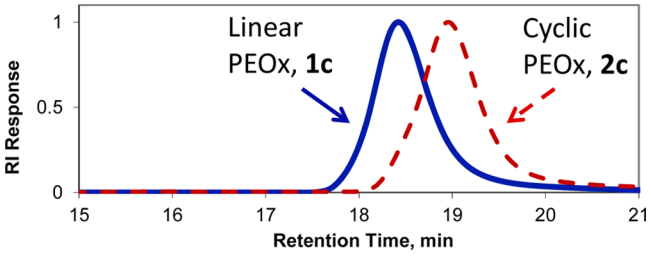

Figure 2. Representative gel permeation chromatography (GPC) traces of linear PEOx (**1c**) precursor and cyclic PEOx (**2c**) product. The increased retention time upon cyclization is characteristic for a successful ring closure. *Mn calculations are based on retention time comparisons against linear polystyrene standards.

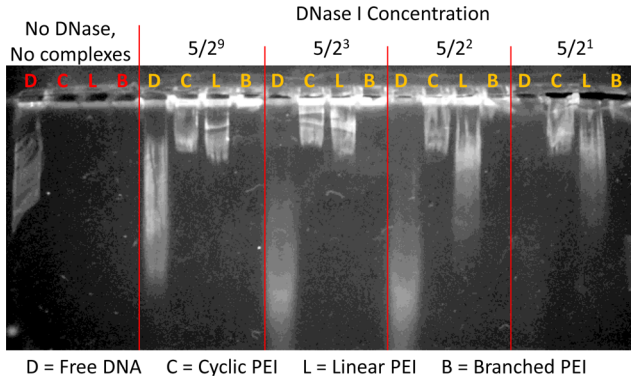

Figure 3. DNA protection and complex stability assay. PEI/DNA complexes were made with cyclic **4d**, linear **3d**, and branched PEI at N:P ratios of 20:1, 20:1, and 7.5:1, respectively, with free DNA serving as a control. Complexes were exposed to DNase I at the indicated concentrations for 3 min, after which the reaction was stopped and the samples were immediately loaded into an alkaline gel to separate the DNA from its carrier.

Figure S2, resonance d) provided further validation of the molecular weight determination by both GPC and MALDI-ToF MS (Table 1, compound **1a**). In addition, MALDI-ToF MS (Figure 1a) and GPC (Figure 2, represented in blue) were used to confirm the very low dispersity ($Đ$) of the linear PEOx samples (1.0−1.1), which is indicative of a polymerization with well-controlled initiation and termination (Table 1, **1a**−**1d**).

The most characteristic data for confirming a successful CuAAC cyclization are the quantitative replacement of the end group functionalities with a triazole linkage, and a reduction in the hydrodynamic volume resulting from the more compact cyclic topology. The loss of the azide end group upon cyclization could be confirmed by the loss of the azide absorbance in the FTIR spectra of **2** (Supporting Information Figure S1b). Likewise, the unique azide metastable fragment which is the major distribution for the linear precursor, **1**, disappears and is replaced by a stable series of macromolecular triazole ions for **2** (Figure 1a,b). ^{1}H NMR was also used to confirm the cyclization by changing end group signals, particularly the appearance of a new triazole resonance at 7.6 ppm (Supporting Information Figure S3, resonance f). Furthermore, the reduction in hydrodynamic radius was confirmed by a shift in the GPC retention time of **2**, relative to the linear precursor, **1**, (Figure 2, represented in red) while

DOI: 10.1021/jacs.5b00980
J. Am. Chem. Soc. 2015, 137, 6541−6549

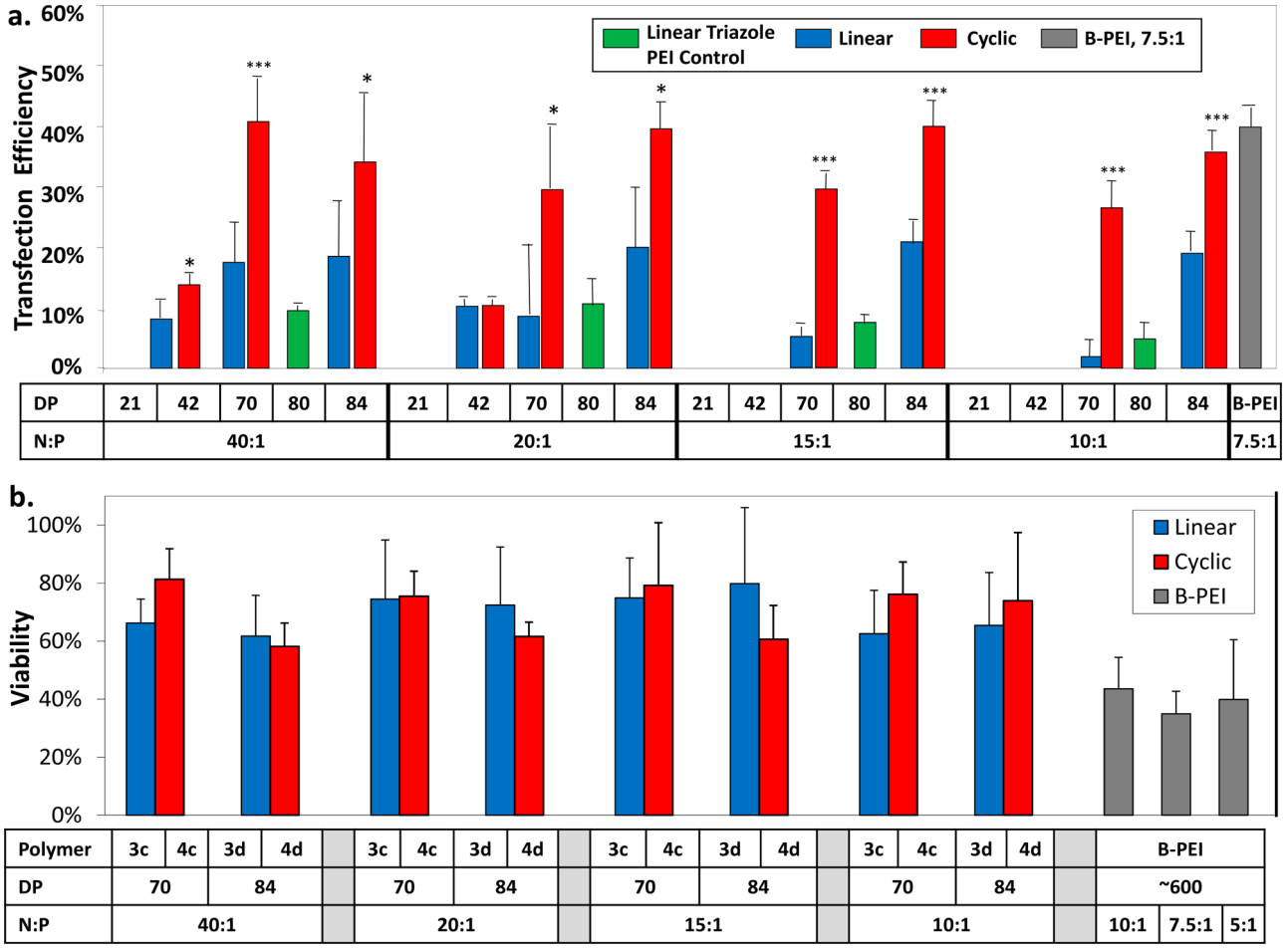

Figure 4. (a) Transfection efficiencies with HFF-1 cells for linear and cyclic PEI at different N:P ratios. (* = Significantly different from the linear version of the same polymer at the same N:P, $P < 0.05$; *** = Significantly different from the linear version of the same polymer at the same N:P, $P < 0.005$) (b) Viability of cyclic polymers **4c** and **4d** normalized to SHAM and branched PEI (B-PEI) at different N:P ratios for HFF-1 cells. There was no difference in means between the normalized numbers of viable cells obtained with polymer **4c** and **4d**, at all N:P tested, and Sham-treated groups (ANOVA, $n \geq 3$ for each group, $P = 0.125$).

retaining its full molecular weight in its mass spectrum (Figure 1b; Table 1, **2a–2d**). This consistent body of data provides convincing evidence for a nearly quantitative cyclization of the linear PEOx, and ^{1}H NMR (Supporting Information Figure S3) integration ratios of the backbone with respect to the triazole signal provide an additional means of confirming the molecular weight (~1900 Da for **2a**) of the cyclic PEOx polymers.

After acid catalyzed hydrolysis, ^{1}H NMR spectra of the PEI products confirmed the complete loss of the side chain signals (Supporting Information Figures S4 and S5) providing strong evidence for the quantitative deacylation, while FTIR confirmed the retention of the azido end group of the linear PEI, **3** (Supporting Information Figure S1c) and ^{1}H NMR confirmed the retention of the triazole linking group for the cyclic PEI, **4** (Supporting Information Figure S5, resonance e).

Although acquiring MALDI-ToF MS data for larger PEI samples proved to be challenging,[42] spectra of the lowest molecular weight samples exhibited the predicted average molecular weight (900), based upon the molecular weight of their PEOx precursors (Figure 1c,d). In addition, consistent patterns of metastable fragment ions for the linear azido-functional PEI samples, and the absence of metastable ions for the cyclic PEI samples confirmed their linear and cyclic architectures, respectively.

PEI Library for Biological Studies. A library that consisted of four sets of linear and cyclic PEI (with 21, 42, 70, and 84 repeat units) was then evaluated as gene delivery agents. To discount any effect that the end groups or trace CuAAC impurities may have on transfection, also included in the transfection study were three linear PEI triazole control samples (with 17, 44, and 80 repeat units) that underwent identical CuAAC coupling conditions to generate a triazole end group but on a *linear* PEI backbone. Because the synthesis of these control samples required a separate polymerization, using a different initiator, the numbers of repeating units were similar, but not identical, to the focus set of linear and cyclic PEI samples (Table 1, **7e–7g**).

DNA Protection and Complex Stability. PEI/DNA complexes were made with the three architectures of PEI, and exposed to DNase I for 3 min. The concentrations of DNase I were varied as indicated in Figure 3. The method of displaying the amount of DNase I is based upon 5 units of the enzyme being diluted 1:2 for this series of experiments. From the figure, it can be seen from the position of the smear in the free-DNA lanes that the unbound DNA is digested more as DNase I concentration is increased (the smear runs faster, indicating smaller fragments), until it is completely digested by exposure to 5/2 U of DNase I for 3 min. It can also be seen that

DOI: 10.1021/jacs.5b00980
J. Am. Chem. Soc. 2015, 137, 6541–6549

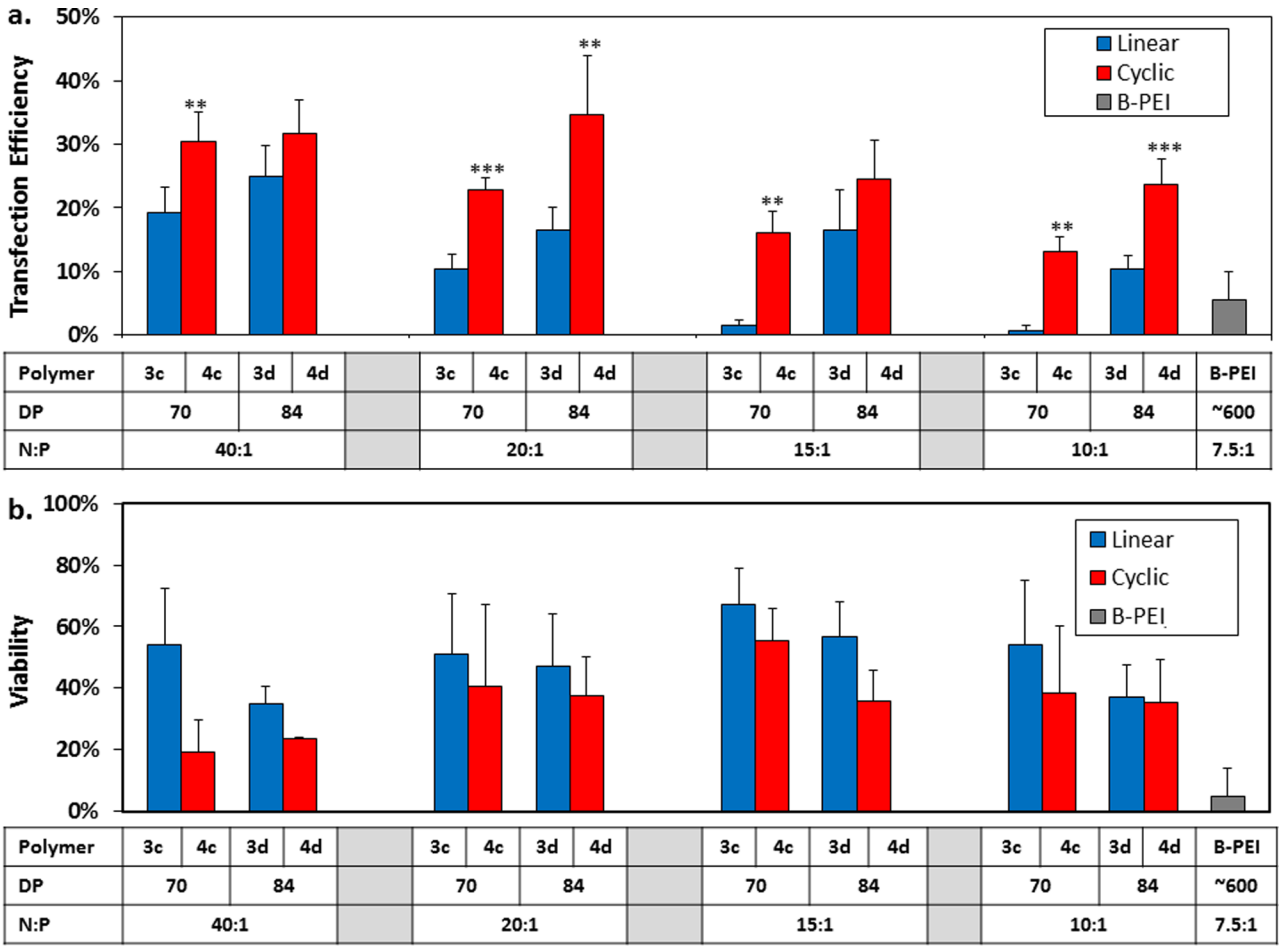

Figure 5. (a) Transfection efficiencies with HAE cells for linear and cyclic PEIs at different N:P ratios. (** = Significantly different from the linear version of the same polymer at the same N:P, $P < 0.01$; *** = Significantly different from the linear version of the same polymer at the same N:P, $P < 0.005$.) (b) Viability for linear, cyclic, and branched PEI at different N:P ratios, normalized to SHAM, at different N:P ratios for HAE cells.

DNA protected by B-PEI remains very well-protected, as shown by the lack of a smear even at 5/2 U of DNase I. Cyclic and Linear PEIs offer some protection, but not as much as branched PEI. The intensity and distance traveled in the gel indicate that cyclic PEI offers more protection to the DNA it carries than does linear PEI of the same size.

Gene Delivery. Transfection studies were performed with the full library of linear PEI, cyclic PEI and linear triazole control PEI samples upon human foreskin fibroblast (HFF-1) cells (ATCC, Manassas, VA) using 25 kDa branched PEI as a positive control (Figure 4a). The best performing cyclic polymers (**4c** and **4d**) and their linear analogues (**3c** and **3d**) were then studied with human aortic endothelial (HAE) cells (Figure 5a). In both studies, the polymers were used to complex and deliver plasmids encoding a red fluorescent protein (pCMV-DsRed- Express, Clontech, Mountain View, CA). It was found that polymers with fewer (21−42) repeat units, such as **3a−b** and **4a−b**, generally did not yield positively transfected cells. On the other hand, polymers of more repeat units (70−84) such as **3c−d** and **4c−d** yielded significant RFP expression.

In general, cyclic polymers showed significantly higher transfection efficiencies of RFP than their linear counterparts and, at optimal N:P ratios (ratio of nitrogen in PEI to phosphorus in DNA), yielded transfection efficiencies comparable to those of the 25 kDa (~600 repeat units) branched PEI positive control.[18,23] The linear PEI triazole control polymer with 80 repeat units (**7g**) generally yielded transfection efficiencies that were similar to those observed for the linear PEIs having 70 (**3c**) and 84 (**3d**) repeat units, suggesting that the substantial increase in transfection observed for the cyclic polymers is a result of PEI architecture rather than a modification of the end group functionalities.

Additional transfection studies with Gaussia luciferase were performed with freshly synthesized batches of **3c** and **4c**, along with a different preparation of branched PEI, to assess the difference in the total amount of gene expressed for the three architectures (Supporting Information Figure S9). Samples of **3d** were included to investigate the differences between increasing molecular weight (**3c** to **3d**) versus changing architecture (**3c** to **4c**). It was found again that the cyclic architecture tended to outperform the linear counterpart in terms of transfection efficiency.

Cell Viability. Viability studies were performed on both HFF-1 and HAE cells using the two best-performing cyclic PEI samples **4c** and **4d** (70 and 84 repeat units) as well as their linear analogues, **3c** and **3d**, and compared with branched PEI of 600 repeat units (Figures 4b and 5b). The cyclic polymers used at the 20:1, 15:1, or 10:1 (or 40:1 for the 84-repeat version) N:P ratios were seen to be significantly less cytotoxic than branched PEI used at a 7.5:1 N:P (ANOVA, $n \geq 3$, $P = 0.0002$). However, there was no significant difference between

DOI: 10.1021/jacs.5b00980
J. Am. Chem. Soc. 2015, 137, 6541−6549

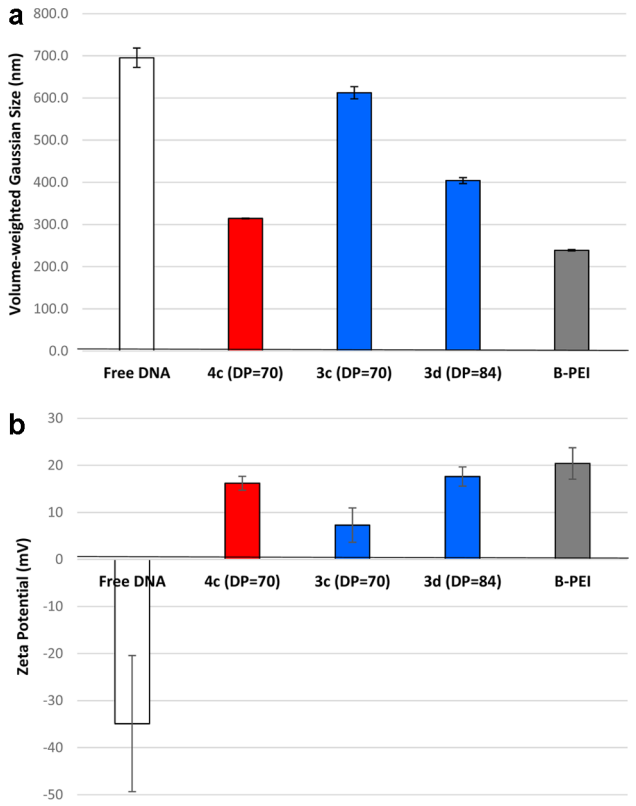

Figure 6. (a) Sizes of transfection complexes, as determined via dynamic light scattering. (b) Zeta potentials of transfection complexes. For both panels, complexes made with cyclic (**4c**) and linear (**3c**, **3d**) PEIs were made at the 40:1 N:P ratio; those using branched PEI were made at 7.5:1.

each cyclic and its linear analogue for each pair of any given molecular weight and N:P (t tests, $P > 0.20$, $n \geq 3$).

Further Characterization. PEI/DNA complexes were made with cyclic, linear, and branched PEIs for comparisons of size (Figure 6a) and surface charge concentration (zeta potential) (Figure 6b). Transfection complexes made with cyclic (**4c**) and linear (**3c**, **3d**) PEIs were made at the 40:1 N:P ratio, and those using branched PEI were made at 7.5:1. It was noted from dynamic light scattering data that DNA was condensed in the presence of each PEI sample. Furthermore, the PEIs that yielded better transfection efficiency (**4c** and B-PEI) also yielding more-condensed DNA. The zeta potentials of the tested PEI/DNA formulations reflected the excess of PEI (N:P > 1), with the branched architecture having a slightly higher average zeta potential, despite having the relatively lower N:P ratio (7.5:1 versus 40:1).

Discussion. The transfection efficiency of the two largest and most promising cyclic polymers (70 and 84 repeat units, depicted in red, Figures 4a and 5a) were compared against their linear analogues at each of four different N:P ratios (40:1; 20:1; 15:1; and 10:1, depicted in blue) in both HFF and HAE cells. For both cell lines, the transfection efficiency was consistently higher for each cyclic PEI than its linear analogue, regardless of N:P ratio and molecular weight, confirming that the cyclic PEI architecture affords a unique advantage in affecting gene delivery. Furthermore, DNA protection (Figure 3) and condensation studies (Figure 6a) show that the cyclic PEI offers more protection and condenses DNA to a smaller size than its linear PEI analogue. The linear PEI triazole control (depicted in green in Figure 4a) sample with 80 repeat units (**7g**) exhibited transfection efficiencies in line with the azido/alkyne functionalized linear PEIs (**3c,d**) with 70 and 84 repeat units, suggesting that the improved transfection observed for the cyclic polymers is not a result of the triazole functionality or any trace contaminants that may remain from the CuAAC reaction. Branched PEI is typically used as a benchmark for transfection,[51,52] so these cyclic and linear PEI data were also compared to a "gold standard" 25 kDa MW branched PEI[18,23] (~600 repeat units) at an optimized 7.5:1 N:P ratio. While the transfection efficiency for branched PEI generally improves with increasing molecular weight,[16,19] the cyclic PEIs with only 70 and 84 repeat units exhibited significantly improved transfection for the HAE cells relative to the optimized, branched PEI (Figure 5a), and performed equally as well as the much larger branched PEI in the case of HFF cells (Figure 4a). These observations together suggest that the cyclic topology may offer a unique advantage with respect to the more traditional linear and branched PEIs for gene delivery applications.

While the exact origin of the cyclic polymers' increased transfection efficiency is still under investigation, there are two significant physical differences between the linear and cyclic analogues that likely play a role. First, the cyclic polymers exhibit a more compact conformation which, when protonated, results in a higher charge density than their linear counterparts. This hypothesis concurs with previously reported studies comparing star and linear PEIs that attribute the improved transfection efficiency of stars to their increased charge density.[26,27] A related physical consequence of the cyclic topology is a reduced flexibility relative to linear analogues, which may have entropic as well as enthalpic consequences for binding DNA. It is proposed, then, that an enhanced interaction with DNA is a major factor in the observed improvement in RFP expression for the cyclic PEI samples. The dynamic light scattering data (Figure 6a) does show the cyclic polymer (**4c**) condensing DNA to a smaller size than its linear analogue (**3c**), which correlates to a PEI sample that yielded higher transfection efficiency. DNA protection analysis also showed greater protection afforded by the cyclic PEIs versus their linear analogues. Interestingly, the cyclic polymers also show minimal changes in transfection efficiencies as N:P ratios are varied, while the analogous linear polymers studied (and the branched PEI polymer, reported elsewhere[12]) show an apparent decreasing transfection efficiency as the N:P ratio is decreased toward 1:1.

Often, factors that improve transfection efficiency, such as increasing molecular weight, also significantly increase toxicity,[16] requiring a practical compromise between these two critical parameters. In general, the cyclic polymers were less toxic than the 25 kDa branched PEI (~600 repeat units), despite the fact that the cyclic polymers were used at much higher N:P ratios. However, more significantly, this study demonstrated that the cyclic PEI exhibits significantly greater transfection efficiency relative to linear analogues (Figures 4 and 5). Compared with the transfection efficiencies of branched PEI controls, the cyclic architecture yielded comparable (or greater, depending on cell type) transfection efficiency *while* exhibiting reduced cytotoxicity, which represents an alternative and exciting approach for simultaneously optimizing these two critical parameters for gene delivery. The reduced toxicity relative to the branched controls is likely a consequence of significantly reduced molecular weight of the cyclic samples.

DOI: 10.1021/jacs.5b00980
J. Am. Chem. Soc. 2015, 137, 6541−6549

However, the full effect of PEI architecture and the triazole functional group on cell viability will require further investigation.

CONCLUSIONS

The synthesis of well-defined cyclic PEI is reported for the first time in this study. This synthetic route enables the production of exact linear analogues from precursors, permitting the systematic correlation of transfection efficiencies relative to polymer architecture. The delivery of genes encoding a red fluorescent protein was explored with 4 different molecular weights of linear and cyclic PEIs, at 4 different N:P ratios. Cyclic PEIs were found to significantly outperform their linear analogues at every molecular weight and N:P ratio. Likewise, the cyclic PEIs also performed as well as, or better than, the current gold standard: 25K branched PEI, but with significantly reduced toxicity. In agreement with previous reported studies, it is believed that the improved transfection efficiencies are, in part, the result of increased charge density resulting from the more compact structure of the cyclic polymers. These studies confirm that the cyclic architecture provides unique advantages for gene delivery and also highlight the value of systematic architectural studies for optimizing polymer-based vectors for gene delivery.

ASSOCIATED CONTENT

Supporting Information

Additional characterization data, including FTIR and ^{1}H NMR data, as well as detailed descriptions of the synthesis, gene transfection and cell viability experiments. The Supporting Information is available free of charge on the ACS Publications website at DOI: 10.1021/jacs.5b00980.

AUTHOR INFORMATION

Corresponding Author

*sgrayson@tulane.edu

Notes

The authors declare no competing financial interest.

ACKNOWLEDGMENTS

The authors acknowledge Tulane University and the NSF (DMR 0844662) for support of this research and the Louisiana Board of Regents for a graduate fellowship (M.A.C.). The authors also acknowledge Profs. Bruce C. Gibb and Daniel F. Shantz for providing instrument access to acquire DLS/zeta potential data as well as Joseph A. Giesen and Ravinder Elupula for assistance.

REFERENCES

(1) Zhang, S.; Zhao, Y.; Zhao, B.; Wang, B. *Bioconjugate Chem.* **2010**, *21*, 1003−1009.
(2) Putnam, D. *Nat. Mater.* **2006**, *5*, 439−451.
(3) Zhang, X.; Godbey, W. T. *Cancer Gene Ther.* **2011**, *18*, 34−41.
(4) Zhang, X.; Turner, C.; Godbey, W. T. *Mol. Biotechnol.* **2008**, *41*, 236−246.
(5) Zhang, X.; Atala, A.; Godbey, W. T. *Cancer Gene Ther.* **2008**, *15*, 543−552.
(6) Pack, D. W.; Hoffman, A. S.; Pun, S.; Stayton, P. S. *Nat. Rev. Drug Discovery* **2005**, *4*, 581−593.
(7) Vile, R. G.; Russell, S. J.; Lemoine, N. R. *Gene Ther.* **2000**, *7*, 2−8.
(8) Kerr, D. *Nat. Rev. Cancer* **2003**, *3*, 615−622.
(9) McNeish, I. A.; Bell, S. J.; Lemoine, N. R. *Gene Ther.* **2004**, *11*, 497−503.
(10) Marshall, E. *Science* **2000**, *288*, 951−957.
(11) Machitani, M.; Yamaguchi, T.; Shimizu, K.; Sakurai, F.; Katayama, K.; Kawabata, K.; Mizuguchi, H. *Pharmaceutics* **2011**, *3*, 338−353.
(12) Boussif, O.; Lezoualc'h, F.; Zanta, M. A.; Mergny, M. D.; Scherman, D.; Demeneix, B.; Behr, J. P. *Proc. Natl. Acad. Sci. U.S.A.* **1995**, *92*, 7297−7301.
(13) Prevette, L. E.; Lynch, M. L.; Reineke, T. M. *Biomacromolecules* **2010**, *11*, 326−332.
(14) Tang, M. X.; Redemann, C. T.; Szoka, F. C. *Bioconjugate Chem.* **1996**, *7*, 703−714.
(15) Parhamifar, L.; Larsen, A. K.; Hunter, A. C.; Andresen, T. L.; Moghimi, S. M. *Soft Matter* **2010**, *6*, 4001.
(16) Godbey, W. T.; Wu, K. K.; Mikos, A. G. *J. Biomed. Mater. Res.* **1999**, *45*, 268−275.
(17) Grayson, S. M.; Godbey, W. T. *J. Drug Targeting* **2008**, *16*, 329−356.
(18) Abdallah, B.; Hassan, A.; Benoist, C.; Goula, D.; Behr, J. P.; Demeneix, B. A. *Hum. Gene Ther.* **1996**, *7*, 1947−1954.
(19) Fischer, D.; Bieber, T.; Li, Y.; Elsasser, H.-P.; Kissel, T. *Pharm. Res.* **1999**, *16*, 1273−1279.
(20) Papisov, I. M.; Litmanovich, A. A. *Adv. Polym. Sci.* **1989**, *90*, 139−179.
(21) Ogris, M.; Steinlein, P.; Kursa, M.; Mechtler, K.; Kircheis, R.; Wagner, E. *Gene Ther.* **1998**, *5*, 1425−1433.
(22) Morimoto, K. *Mol. Ther.* **2003**, *7*, 254−261.
(23) Thomas, M.; Klibanov, A. M. *Proc. Natl. Acad. Sci. U.S.A.* **2002**, *99*, 14640−14645.
(24) Merkel, O. M.; Mintzer, M. A.; Sitterberg, J.; Bakowsky, U.; Simanek, E. E.; Kissel, T. *Bioconjugate Chem.* **2009**, *20*, 1799−1806.
(25) Xu, F. J.; Zhang, Z. X.; Ping, Y.; Li, J.; Kang, E. T.; Neoh, K. G. *Biomacromolecules* **2009**, *10*, 285−293.
(26) Nakayama, Y. *Acc. Chem. Res.* **2012**, *45*, 994−1004.
(27) Cai, X.; Dong, C.; Dong, H.; Wang, G.; Pauletti, G. M.; Pan, X.; Wen, H.; Mehl, I.; Li, Y.; Shi, D. *Biomacromolecules* **2012**, *13*, 1024−1034.
(28) Georgiou, T. K. *Polym. Int.* **2014**, *63*, 1130−1133.
(29) *Cyclic Polymers*; Semlyen, J. A., Ed.: Kluwer Academic Publishers: Dordrecht, The Netherlands, 2000.
(30) Laurent, B. A.; Grayson, S. M. *Chem. Soc. Rev.* **2009**, *38*, 2202.
(31) Zhu, Y.; Gido, S. P.; Iatrou, H.; Hadjichristidis, N.; Mays, J. W. *Macromolecules* **2003**, *36*, 148−152.
(32) Lescanec, R. L.; Hajduk, D. A.; Kim, G. Y.; Gan, Y.; Yin, R.; Gruner, S. M.; Hogen-Esch, T. E.; Thomas, E. L. *Macromolecules* **1995**, *28*, 3485−3489.
(33) Hadjichristidis, N.; Pitsikalis, M.; Pispas, S.; Iatrou, H. *Chem. Rev.* **2001**, *101*, 3747−3792.
(34) Nasongkla, N.; Chen, B.; Macaraeg, N.; Fox, M. E.; Fréchet, J. M. J.; Szoka, F. C. *J. Am. Chem. Soc.* **2009**, *131*, 3842−3843.
(35) Chen, B.; Jerger, K.; Fréchet, J. M. J.; Szoka, F. C. *J. Controlled Release* **2009**, *140*, 203−209.
(36) Laurent, B. A.; Grayson, S. M. *J. Am. Chem. Soc.* **2006**, *128*, 4238−4239.
(37) Hoskins, J. N.; Grayson, S. M. *Macromolecules* **2009**, *42*, 6406−6413.
(38) Eugene, D. M.; Grayson, S. M. *Macromolecules* **2008**, *41*, 5082−5084.
(39) Wei, H.; Chu, D. S. H.; Zhao, J.; Pahang, J. A.; Pun, S. H. *ACS Macro Lett.* **2013**, *2*, 1047−1050.
(40) Aoi, K. *Prog. Polym. Sci.* **1996**, *21*, 151−208.
(41) Kobayashi, S.; Tokuzawa, T.; Saegusa, T. *Macromolecules* **1982**, *15*, 707−710.
(42) Lambermont-Thijs, H. M. L.; van der Woerdt, F. S.; Baumgaertel, A.; Bonami, L.; Du Prez, F. E.; Schubert, U. S.; Hoogenboom, R. *Macromolecules* **2010**, *43*, 927−933.
(43) Cortez, M. A.; Grayson, S. M. Polyplex Gene Delivery Vectors. U.S. Patent 2013/0115699 A1, 21 March 2011.
(44) Wiesbrock, F.; Hoogenboom, R.; Abeln, C. H.; Schubert, U. S. *Macromol. Rapid Commun.* **2004**, *25*, 1895−1899.

DOI: 10.1021/jacs.5b00980
J. Am. Chem. Soc. 2015, 137, 6541−6549

(45) Li, Y.; Hoskins, J. N.; Sreerama, S. G.; Grayson, S. M. *Macromolecules* **2010**, *43*, 6225−6228.
(46) De la Rosa, V. R.; Bauwens, E.; Monnery, B. D.; De Geest, B. G.; Hoogenboom, R. *Polym. Chem.* **2014**, *5*, 4957.
(47) Adams, N.; Schubert, U. S. *Adv. Drug Delivery Rev.* **2007**, *59*, 1504−1520.
(48) Thomas, M. *Proc. Natl. Acad. Sci. U.S.A.* **2005**, *102*, 5679−5684.
(49) Tomalia, D. A.; Sheetz, D. P. *J. Polym. Sci., Part A-1: Polym. Chem.* **1966**, *4*, 2253−2265.
(50) Li, Y.; Hoskins, J. N.; Sreerama, S. G.; Grayson, M. A.; Grayson, S. M. *J. Mass Spectrom.* **2010**, *45*, 587−611.
(51) Wang, J.; Lei, Y.; Xie, C.; Lu, W.; Yan, Z.; Gao, J.; Xie, Z.; Zhang, X.; Liu, M. *Int. J. Pharm.* **2013**, *458*, 48−56.
(52) Fu, C.; Lin, L.; Shi, H.; Zheng, D.; Wang, W.; Gao, S.; Zhao, Y.; Tian, H.; Zhu, X.; Chen, X. *Biomaterials* **2012**, *33*, 4589−4596.

DOI: 10.1021/jacs.5b00980
J. Am. Chem. Soc. 2015, 137, 6541−6549